Plasma Suppression of Diesel Soot Deposition During Diesel Engine Operations

J. S. Chang[1], C. Luthereau[1,2], E. dela Cruz[1], P. I. Khalaf[1,3], D. Brocilo[1], G. D. Harvel[1,4], D. Ewing[1], N. A. Debacher[3], F. McCluskey[2], J. S. Cotton[1,5] and M. Bardeleben[5]
[1] McIARS, McMaster University, Canada
[2] IOT, Université Joseph Fourier, France
[3] Federal University of Santa Catalina, Brazil
[4] University of Ontario Institute of Technology, Canada
[5] Dana Corp, Long Mfg Inc., Canada

Abstract—This About 40 % of the air pollution is generated by vehicles and transports. The particulate matter (PM) emission significantly impacts human health. Fine particles below 2.5 μm (PM2.5) can enter the lungs and lead to respiratory problems. These particles not only influence human health, but also reduce the capability of many au-tomobile exhaust heat exchanging devices, such as exhaust gas recirculation (EGR) cooling systems and corro-sion problems in exhaust systems of a diesel engine, since the soot deposit layer acts as thermal isolation and adsorbs corrosive gases. This study examines using non-thermal plasma systems to prevent significant formation and deposition of soot. An experiment was conducted to suppress soot deposition to the pipe wall by non-thermal plasma generated radicals, metastables and ions. The results show that the chemical oxidation and reduction that occur during the plasma process may suppress soot deposition on the pipe wall since some soot oxidation and ash reduction gaseous by-products were observed. Non-thermal plasma also contributed a removal of NOx and CO from the diesel exhaust. The physical suppression of soot deposition is also observed, since soot layer thickness in the pipe wall is relatively uniform which may be due to the re-entrainment of the deposited soot and effect of electrohydrodynamic flow.

Keywords—Diesel Soot Removal, Non-thermal Plasma, Flow Stabilized Corona, Electrohydrodynamics, Neutron Radiography Imaging

I. INTRODUCTION

Atmospheric pollution is becoming an increasingly important issue worldwide, especially pollution created from the burning of hydrocarbon fuels. A pollutant often overlooked is particulate matter in the form of soot. Particulate matter can be very hazardous to human health and hence a reduction of soot emissions is essential. Plasma oxidation of deposited soot was developed to reduce the amount of soot emissions (Harano et al. [18, 21],Yao et al. [17], Brocilo et al. [5], Ohkubo et al. [8], Grundmann et al. [20], Martin et al. [2]). In the experimental and modeling study of soot oxidation by Martin et al. [2], the erosion of soot by oxidation in a non-thermal, atmospheric pressure plasma has been modeled using a simplified, two layer, kinetic scheme for the surface reactions coupled with a gas-phase reaction mechanism that is appropriate to diesel exhaust gas. The proposed reactions by Martin et al. [2] are shown in Table 1. The experimental measurements in this work were limited to measuring the carbon erosion rate and the evolution of CO and CO_2 in order to validate the model. This modeling was developed in a step-wise and systematic manner to explain the experimental results. The model represents the soot as two distinct layers. The chemistry which leads to carbon erosion by heterogeneous oxidation takes place only in the outer surface layer (C_s). The second layer is an inner or bulk layer which contains most of the mass of the soot (C_b). Site vacancies in the outer layer (X_s) are immediately replaced by carbon from the inner bulk layer (reaction 5). Soot that is deposited from the gas phase as elemental carbon is absorbed into the sub-surface bulk layer (reaction 6). The oxidation or erosion rate of the soot is given by the change in the mass of bulk layer as function of time. This model reproduces the surface to volume ratio of the experiment.

TABLE I
PROPOSED REACTIONS BY MARTIN ET AL. [2]

	Reactions
1	$C_s + O \rightarrow CO_s$
2	$C_s + C_s + O_2 \rightarrow CO_s + CO_s$
3	$CO_s \rightarrow CO + X_s$
4	$CO_s + CO_s \rightarrow CO_2 + C_s + X_s$
5	$C_b + X_s \rightarrow C_s$
6	$C \rightarrow C_b$
7	$C_s + OH \rightarrow CO_s + H$
8	$C_s + NO_2 \rightarrow CO_s + NO$
9	$C_s + O_3 \rightarrow CO_s + O_2$

TABLE II
PROPOSED ADDITIONAL REACTIONS BY BROCILO ET AL. [5]

	Reactions
1	$C_s + O_2{}^{*} \rightarrow CO_2$
2	$C_s + 2NO \rightarrow NO_2$
9	$C_s + Y^{-}$ or $^{+}$ --> CY^{-} or $^{+}$

Corresponding author: J. S. Cotton
e-mail address: cottonjs@mcmaster.ca

Presented at the 6th International Conference on Applied Electrostatics in November 2008, Accepted: February 3, 2009

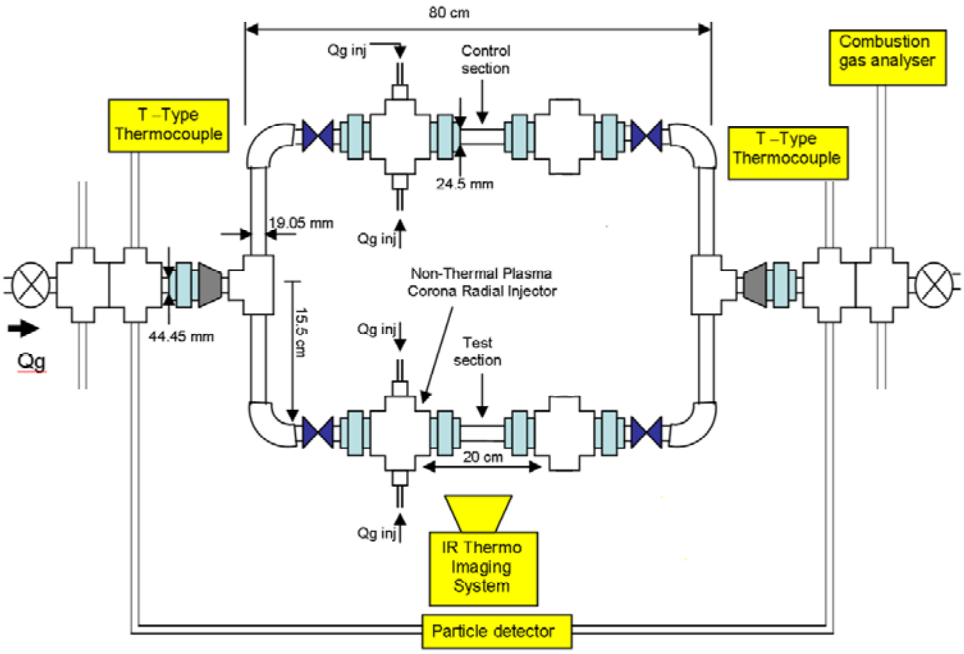

Fig. 1. Schematic of plasma soot oxidation experimental set up and apparatus.

Brocilo et al. [5] examined plasma soot oxidation and proposed that other reactions initiated by metastables (*), negative (Y^-) and positive (Y^+) ions might take place in addition to the reactions proposed by Martin et al.. Wick et al.'s [3] previous work on soot oxidation chemistry showed substantial net adsorption of oxygen atoms by the soot. In this work, the gaseous combustion products, CO_2 and CO, were measured using a mass spectrometer, while the weight change of the soot was monitored by a microbalance. Under their experimental conditions, they found that the soot adsorbed up to 25 % by weight oxygen, compared to an initial soot composition of less than 5 % by weight oxygen. This is a chemical adsorption, in which the oxygen atoms are strongly bonded to carbon atoms in the soot. Statistically, this 25 % oxygen content corresponds to one oxygen atom for every four carbon atoms in the soot. Wick et al. [4] also observed that nitric oxide inhibits the rate of soot oxidation by oxygen atoms at 298 K. Small amounts of added NO reduced the rates of production of CO_2 and CO by up to 35 %. It was shown experimentally that NO was not reducing the gas phase O atom concentration. Thermal desorption mass spectrometry showed a small adsorption of NO on the soot. This inhibition is interpreted in terms of a relatively small number of reactive sites on the soot at which soot gasification occurs and which are effectively blocked by NO.

The corona discharge in the plasma usually generates a strong electrohydrodynamic (EHD) flow sometimes called an ionic or electric wind (Chang and Watson [26]). This EHD wind may also suppress the deposition of the soot particles due to convection and re-entrainment (Beuthe and Chang [1]). The soot particles may be electrically charged during the combustion process (Mariq [22]) and these charged soot particles may be further neutralized by the positive and negative ions in the plasma, hence the deposition of the soot may be further reduced.

The objective of this work was to determine whether the plasma method was effective to reduce formation and deposition of soot from diesel exhaust gases. The experiments were performed in the near zero emission diesel engine (NZEDE) test facility. The real time neutron radiography system was used to non-destructively measure deposited soot thickness distribution.

II. EXPERINTAL APPARATUS

The experiments were performed in the near zero emission diesel engine exhaust test facility [5] that consists of a diesel engine and pollution control system connected to the engine exhaust gas pipe. Located in a sound reducing shielded enclosure, a single cylinder Lombardini 15LD 350 diesel engine was connected to a 5.5 kW Lombardini generator. The load is created electrically with a variable resistance. The fuel consumption is approximately 18.75 mL /min, for a load of 2.5 kW. The main exhaust gas pipe, which is 44.45 mm (1 ¾") diameter pipe, splits into the test and by-pass branches each equipped with the venturi flow meter. The branches rejoin before a diesel particulate filter followed by an electrical heater and a catalytic converter.

The tests were performed using two corona discharge oxidation reactor legs in parallel as shown in Fig. 1.The portion of the main diesel exhaust flow (Qg) enters on the left side in Fig.1 and then splits into a control section and a test section. The test and control sections consists of a 20 cm long, 25.4 mm (1”) diameters pipe with two flow stabilized corona non-thermal plasma reactors (Maezono and Chang [23]) at either end, in the current research only the upstream plasma reactors are enabled. The test pipe extends into the non-thermal plasma reactor to the nozzle tip so that the visible part is only 15 cm long. The test pipe is composed of aluminium and can be analysed via real-time nuclear radiography (RTNR) (Ismail et al. [24, 25]) without significant neutron attenuation. The non-thermal plasma corona radial injection consists of a stainless steel tube placed perpendicular to the main gas flow with two 1.58 mm (1/16”) diameter 10 mm long nozzles that act as the electrodes. The electrode dimensions have been chosen to avoid electrical discharge on the main body. This tube and nozzles arrangement act as the electrode where the high voltage is applied. The corona generated has a shape of a fan beginning at the nozzle. The electrode is insulated from the cross section by a Teflon part, and the cross-section is grounded. The injected air (with a flow of Qg-inj) is introduced in four upstream non-thermal plasma reactors, but the high voltage is only applied to the electrodes in the test section. The injected air is measured via a 20 L/min air rotameter of accuracy 0.2 % full scale. This creates the same flow condition in both sections to be able to compare the effect of the non-thermal plasma oxidation on soot deposition and represents a total dilution rate of less than 5 %. The high voltage applied to the electrodes can be either pulse high voltage or dc high voltage.

In this work, the high voltage pulsed system (Brocilo et al. [5]), driven by triggering circuit dc 24 V power supply on a primary side and an automobile ignition coils on a secondary side, was connected to the high voltage electrodes. Both voltage and current are slightly ringing waveforms due to the mismatching of the discharge generated plasma impedances. Discharge characteristics of non-thermal plasma reactors, when tested with various air injection gas flow rates at a main air flow rate of 0 L/min and 100 L/min, showed that the main air flow rate does not significantly influence the discharge current.

The temperature of the exhaust gas was measured using two T-Type copper/nickel alloy thermocouples with a range of -200 °C to 350 °C, one upstream before the main leg split and one downstream after the flow from the two smaller legs rejoined.

The particle measurement system was designed to alternate between the upstream and downstream locations via directional valve to which an intermediate chamber was installed in order to lower the temperature of the gas sample before connecting to a HAZ-DUST III, real-time personal soot monitor. The particle detector operating range is 0.01 to 200 mg/m^3 and the operating temperature range is from 0 °C to 50 °C.

The combustion gas analyse of the filtered exhaust gas upstream and downstream of the combined test and control branch flow was measured using a GreenLine 8000 combustion gas analyzer (Eurotron Inc.) that can measure the concentrations of CO, NO, NO_2, NOx, SO_2, CO_2, H_2S, O_2, CO, CO_2, and total CxHy. The operation temperature range of the Greenline 8000 is from 5 °C to 45°. The Greenline 8000 has a detection limit for O_2 is 0.01 %, CO_2 is 0.2 % and 1 ppm for CO, NO_x, NO_2, SO_2 and H_2S.

A soot deposition was measured by using a nondestructive neutron imaging system, designed by McMaster and installed in the McMaster Nuclear Reactor Neutron Radiography Facility. The technique uses the ability of the neutrons to transmit through metals but be attenuated by carbon and hydrogen based materials (such as soot).

A high speed infra-red thermography system is used to measure the surface temperature of the test pipe during the experiment. This measurement is useful when analyzing any soot deposition due to the thermophoresis effects.

III. RESULTS AND DISCUSSIONS

The experiments were initiated by allowing the exhaust flow to the test loop 15 minutes after diesel engine operation then the plasma reactors were operated. The measurements were started 10 minutes after the plasma reactors were operated to ensure a stable discharge after which the thermal imaging of the sooted tubes was performed every 15 minutes. The experiments are conducted at the operating conditions summarized in Table 3.

The engine gas composition upstream of the test and

TABLE III

SUMMARY OF THE CHARACTERISTICS FOR THE SOOT DEPOSITION TEST.

System	Parameters
Diesel engine exhaust	Exhaust temperature : 250 °C Main exhaust flow rate : 40 kg/h Test & Control flow rates :10 kg/h each
Primary side power system	Primary side frequency : 200 Hz Primary side voltage : 6 V
Air injection through NTP.	Nozzle velocity of 30 m/s 4 Nozzles each (3.56 L/min.).
Diesel generator load	Voltage : 123 V Current : 20.4 A Engine power : 2.5 kW

TABLE IV

ENGINE EXHAUST GAS COMPOSITION UPSTREAM OF THE TEST AND CONTROL BRANCHES AT TABLE 3 CONDITIONS.

Gas	Upstream Concentration
O_2	12.7 to 13.9 %
CO_2	5.5 to 6.4 %
H_2S	0 ppm
SO_2	0 ppm
CO	521 to 850 ppm
NO_2	5 to 12 ppm
NO_X	415 to 532 ppm
NO	421 to 500 ppm
PM	94 – 144 mg/m^3

control branches, mainly O_2, CO, CO_2, NO_X, NO and particulate matter (PM) concentrations, was dependent on the load condition. Table 4 presents the range of concentration for the system characteristics at steady state under Table 3 conditions. The plasma reactors are turned OFF after 1 hour 30 minutes after the start of the measurements and the diesel engine was turned off 5 minutes after that.

Although the maximum voltage has been kept constant, the exponential decrease in the maximum discharge power throughout the 90 minutes of operation has been observed. The maximum discharge power started from 40 W and than kept decreasing until finally becoming stable at 4 W at t = 60 minutes after which it remained constant until the end of the experiment. This might be due to the observed soot build-up on the electrode surface as well as inner surface of non-thermal plasma reactor.

The concentration of the exhaust gas components during the above 90 minutes of operation are shown in Fig. 2. Fig. 2a shows the transient oxygen concentration in the exhaust downstream of the test section. The oxygen concentration started from 21 % due to the trapped air in the system from start up (t = 0 when exhaust gas bypass open to test section) and then fluctuated around 16.6 % from 0 to 12 minutes due to the operational transient of the loop. The concentration finally became stable with diesel exhaust at a value of 15.1±0.4 % at t =14 minutes and then remained almost constant (mean 15 %) until the end of the experiment. A portion of the increase, approximately 13 %, of the observed increase is due to the ~5 % air dilution of the exhaust stream in test and control section. The additional oxygen content may due to plasma oxidation/reduction reactions with gas composition components including CO, CO_2, NO_X, $H_xC_yO_z$ etc. in exhaust gas [27-34] and adsorbed in soot layer (carbon and hydrocarbons). Fig. 2a also shows the concentration of carbon dioxide (CO_2) measured downstream of the test section. The CO_2 concentration was relatively constant at 3.1 % from 0 to 12 minutes, before increasing to 4.3 % at 13 minutes and remaining relatively stable until 27 minutes. After that, the CO_2 concentration dropped to 0 % until the end of the experiment. This may due to a problem with soot deposition in the IR sensor line. The upstream CO_2 concentration is around 4.1 to 4.3 %.

Fig. 2b shows the concentration of CO in the diesel combustion exhaust measured at downstream of the test section. The carbon monoxide concentration was approximately 188 ppm from 0 to 6 minutes before it increased steeply from 248 ppm (t = 7 min) to 465 ppm (t = 62 min). The gaps of zero concentration in this figure are due to the zero error adjustment of the combustion gas analyzer due to soot deposition. The CO concentration from the diesel exhaust is approximately 350-400 ppm hence enhanced CO_x (x = 1 to 2) detected in the downstream may be due to the oxidation of the soot by O_x (x = 1 to 3 for neutrals and 1 to 6 for ions) radicals, metastables, positive ions and negative ions as proposed by Brocilo et al. (2005).

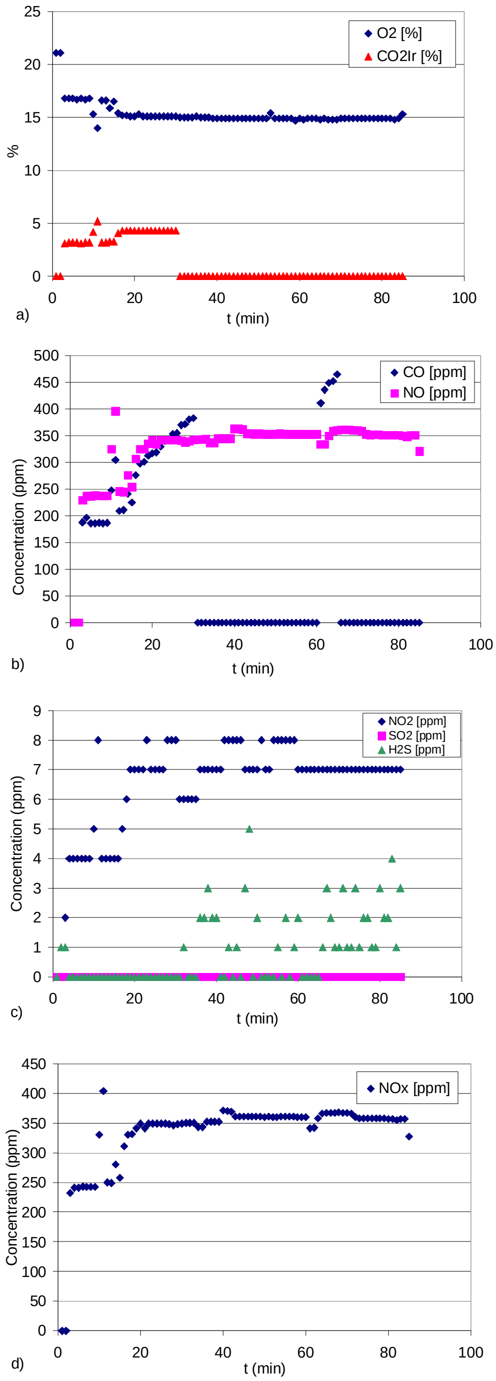

Fig. 2. Gas concentration as function of time for: (a) O_2 & CO_2 in percentage, (b) CO & NO, (c) NO_2, SO_2 & H_2S and (d) NOx (t=0 when exhaust gas by-pass to test section is first opened)

Fig. 2b shows also the transient nitrogen oxide measured at the downstream test section. The NO concentration kept an almost constant value of 237 ppm from 0 to 6 minutes. Then, the NO concentration increased to 342 ppm, in the 7 to 17 minutes range. From 17 to 36 minutes, the (NO) was approximately 342 ppm. At 37 minutes, the emission increased slightly, keeping the values around 353 ppm.

Fig. 2c shows the transient nitrogen dioxide (NO_2), sulphur dioxide (SO_2) and hydrogen sulfide (H_2S) concen- tration during the experiment, measured at the downstream test section. From 0 to 13 minutes, the nitrogen dioxide concentration kept a constant value of 4 ppm. Then it slightly increased to 7 ppm in t = 16 minutes. After that, the nitrogen dioxide concentration oscillated moderately between the values of 6 and 8 ppm until the end of the experiment. The SO_2 concentration kept a constant value of 0 ppm during all of the experimental period. Fig. 3c shows the hydrogen sulfide transient during the experiment, measured at the reactor downstream section. The hydrogen sulfide concentration maintained a constant value of 0 ppm from 0 to 28 minutes. Then it varied slightly from 0 to 5 ppm during the 28 - 62 minutes interval. After this point, the hydrogen sulfide concentration oscillated from 1 to 4 ppm until the end of the experiment. Since the present diesel fuel contains 30 ppm of fuel sulphur, sulphate in ashes will be formed at combustion. Plasma may reduce this sulphate by hydrogen or hydrocarbon radicals formed from the exhaust gases, where no hydrogen sulfide and SO_2 was observed in the upstream diesel exhaust.

Fig. 2d show a total concentration of NOx, where NOx is fluctuating around 350 to 370 ppm. Based on the upstream diesel exhaust NOx concentration of 420 to 480 ppm, the effect of plasma gas phase reaction with the presence of soot is still contributing a small amount of NOx removal, in spite of NOx generation expected from the soot adsorbed NOx and nitrogen and nitrate in ashes. Here the oxidation of soot by NO_2 is not affected by the budget of NOx due to conversion to NO at soot surface as proposed in the Table I.

Fig. 3 shows transients of total hydrocarbon, where a significant 10 to 80 ppm hydrocarbon concentration was observed downstream of the plasma reactor. These hydrocarbons may be generated from the plasma soot surface reactions. The adhesive properties of soot layer may be also reduced by the removal of hydrocarbon from the soot surface as observed in Fig. 4.

The RTNR imaging was used for the soot thickness measurement (Ismail et al. [24, 25]). The RTNR images are taken after the experiment, which corresponds to the diesel engine operation for one and half hours simultaneously with and without the plasma treatment (non-thermal plasma radial injection reactors). The inlet concentration of soot fluctuates between 105 to 131 mg/m^3 and the exhaust gas temperature is fluctuating between 250 and 260 ^{o}C. The RTNR images with and without plasmas are shown in Figs. 4a and 4b, respectively. The soot visualized on the image corresponds to two surfaces. Fig. 4 shows that, the soot deposition is noticeable, particularly on the upstream ending of the test section. A significant amount of soot deposition is on the side borders, as the test section is a cylinder and the integral along the neutron beam path is greatest at the edge. Fig. 4 also shows that the soot deposition is clearly asymmetric and contains 3-dimensional structures. The high concentration on the top part of the cylinder in the image is due to the fact that in the experimental loop, it corresponds to the bottom surface of the cylinder, which may be re-entrained and deposited again by gravity drop-off. By comparison with the control side of image, the results show the plasma treatment was efficient in soot build-up suppression. The area average of the soot deposition thickness, the plasma side and control (without plasma) side are 0.33 and 0.48 mm, respectively. Convective soot transportation may

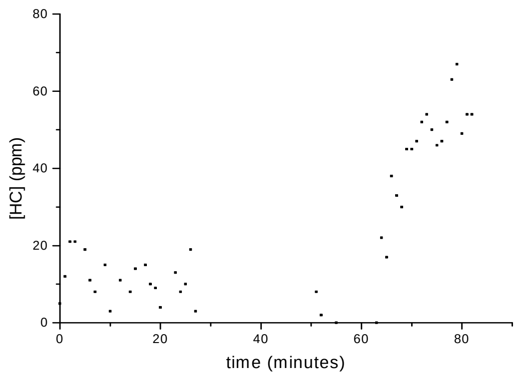

Fig. 3. Transient hydrocarbon concentration measured at downstream test section under diesel exhaust.

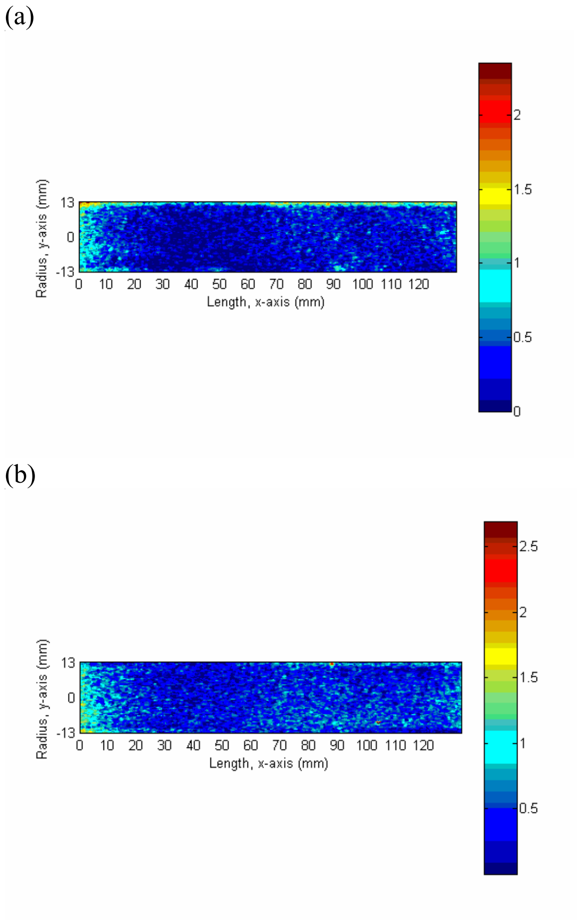

Fig. 4. RTNR image of soot thickness (mm) the exhaust pipe at after 90 min. of diesel operations (a) with plasma; (b) without plasma (control).

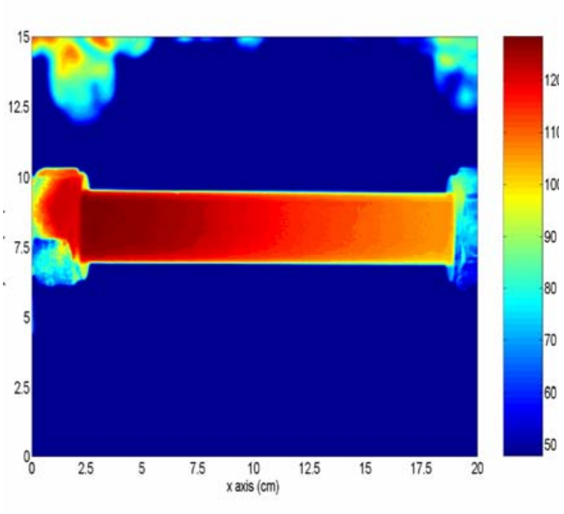

Fig. 5. Infrared image of test section temperature profile (ºC) after 90 min of diesel engine operation.

also be enhanced by EHD gas flow resulting in more uniform soot wall depositions.

The concentration of soot deposition can also be explained to an extend by observing the infra-red thermography image surface temperature distribution as shown in Fig.5. Here the temperature distribution profile, with or without plasma corresponds the soot layer distribution, hence, the deposition is a result of temperature gradients inside a cylindrical section by thermopheresis soot depositions as expected (Beuthe and Chang [1], Ismail et. al. [24]).

IV. CONCLUSIONS

An experiment was conducted to suppress soot deposition to the pipe wall by non-thermal plasma generated radicals, metastables and ions. The results show that the chemical oxidation and reduction that occur during the plasma process may suppress soot deposition on the pipe wall since some soot oxidation and ash reduction gaseous by-products were observed. Non-thermal plasma also contributed to small removal of NOx from the diesel exhaust. The physical suppression of soot deposition is also observed, since soot layer thickness in the pipe wall is relatively uniform which may be due to the re-entrainment of the deposited soot. However, due to the significant soot deposition to the plasma discharge electrode, plasma generation decreases with increasing time. Better optimization of the plasma devices are recommended for future work.

ACKNOWLEDGMENT

Authors thank E. Gerges, J. Burgers, B. Rai, and K. Urashima for valuable discussion and comments. The authors also thank D. Moule for technical assistance. This work is supported by OCE Inc-E-Tech program , Dana Corp., Dophine Prefecture (CL, FM, GDH, JSC) and CNPq (PK, ND, JSC).

REFERENCES

[1] T. G. Beuthe and J. S. Chang, “Gas Discharge Phenomena,” in *Handbook of Electrostatic Process*, J. S. Chang, A. J. Kelly, and J. M. Crowley, Ed. Marcel Dekker, Inc. 1995, ch. 8.

[2] A. R. Martin, J. T. Shawcross, “Whitehead, J. C.; The oxidation of carbon soot in a non-thermal, atmospheric pressure plasma: Experiment and modeling,” *J. Adv. Oxidation Tech.*, vol. 8, no. 2, pp. 126-132, 2005.

[3] B. G. Wicke, C. Wong, and A. G. Karen, “Room temperature oxidation of soot by oxygen atoms,” *Combustion and Flame*, vol. 66, no. 1, pp. 37-46, 1986.

[4] B. G. Wicke, and A. G. Karen, “Nitric oxide inhibition of soot oxi-dation by oxygen atoms at 298K,” *Combustion and Flame*, vol. 69, no. 2, pp. 185-192, 1987.

[5] D. Brocilo, J. S. Chang, D. Ewing, K. Urashima, and J. S. Cotton, “Plasma Removal of Wall Deposited Diesel Soot,” in *Proc. ISPC-17*, pp. 1187-1188, 2005.

[6] S. A. Zhdanok, G. M. Vasil’ev, V. A. Vasetskii, and A. V. Khavets, “Use of Plasma Reforming Fuel for Reduction of the Toxicity of Diesel Engines,” *J. Engineering Physics and Thermophysics*, vol. 78, no. 1, pp. 171–173, 2005.

[7] K. Urashima and J. S. Chang, "Removal of Volatile Organic Compounds from Air Streams and Industrial Flue Gases by Non-Thermal Plasma Technology," *IEEE Trans. Dielectric and Electrical Insulation*, vol. 7, pp. 602-614, 2000.

[8] M. Okubo, T. Kuroki, Y. Miyairi, and T. Yamamoto, “Low-Temperature Soot Incineration of Diesel Particulate Filter Using Remote Non-thermal Plasma Induced by a Pulsed Barrier Discharge,” *IEEE Transactions on Industry Applications*, vol. 40, no. 6, pp. 1504-1512, 2004.

[9] J. Hoard and M. L. Balmer, “Plasma Catalysis for Diesel Nox Remidiation,” *J. Adv. Oxidation Tech.*, vol.4, no. 4, pp. 417-433, 1999.

[10] D.B. Kittelson, “Engines and Nanoparticles: a Review,” *J. Aerosol Sci.*, Vol. 29, No.5/6. (1998). 575-588.

[11] A. Messerer, D. Rothe, U.Pöschl, and R. Niessner, “Advances in the Development of Filterless Soot Deposition Systems for the Continuous Removal of Diesel Particulate Matter,” *Topics in Catalysis*, vols. 30/31, pp. 247-250, 2004.

[12] S. J. Harris and M. M. Maricq, “Signature Size Distributions for Diesel and Gasoline Engine Exhaust Particulate Matter,” *J. Aerosol Sci.*, vol. 32, pp. 749-764, 2001.

[13] K. Donghee, G. Mridul and G. Dinesh, “Parametric Studies on the Formation of Diesel Particulate Matter vie Nucleation and Coagulation Modes,” *J. Aerosol Sci.*, vol. 33, pp. 1609-1621, 2002.

[14] M. Higashi and K.-I. Fujii, “Treatment of Exhaust Gas from Vehicles by Discharge Plasma Reactor,” *Electrical Engineering in Japan*, vol. 120, no.2, pp. 868-872, 1997.

[15] H. Burtscher, S. Kunzel, and C. Hunglin, “Characterization of Particles in Combustion Engine Exhaust,” *J. Aerosol Sci.*, vol. 29, no. 4, 1998.

[16] J. M. Desantes, V. Bermúdez, J. M. García, and E. Fuentes, “Effects of current engine strategies on the exhaust aerosol particle size distribution from a Heavy-Duty Diesel Engine” *J. Aerosol Sci.*, vol. 36, pp. 1251–1276, 2005.

[17] S. Yao, M. Okumoto, and T. Yashima, “Diesel Particulate Matter ad NOx Removals Using a Pulsed Corona Surface Discharge,” *AIChE J.*, vol. 50, no. 3, pp. 715-721, 2004.

[18] A. Harano, M. Sadakata, and M. Sato, “Soot Oxidation in a Silent Discharge,” *J. Chemical Engineering of Japan*, vol. 24, no. 1, pp. 100-106, 1991.

[19] M. Higashi, S. Uchida, N. Suzuki, and K.-I. Fujii, “Soot Elimination and NO, and SO, Reduction in Diesel-Engine Exhaust by a Combination of Discharge Plasma and Oil Dynamics,” *IEEE Transactions on Plasma Science*, vol. 20, no. 1, pp. 1-12, 1992.

[20] J. Grundmann, S. Müller, and R.-J. Zahn, “Treatment of Soot by Dielectric Barrier Discharges and Ozone,” *Plasma Chemistry and Plasma Processing*, vol. 25, no. 5, pp. 455 – 466, 2005.

[21] A. Harano, K. Murata, K. Takamizawa, and M. Sadakata, "Oxidation of Carbonaceous Particles in Silent Discharge Reactor," *J. Chemical Engineering of Japan*, vol. 31, no. 5, pp. 700-705, 1998.

[22] M. M. Mariq, "On the Electrical Charge of Motor Vehicle Exhaust Particles," *J. Aerosol Sci.*, vol. 37, pp. 858-874, 2006.

[23] I. Maezono and J.S. Chang, "Flow Enhanced Corona Discharge-Corona Torch," *J. Appl. Phys.*, vol. 59, pp. 2322-2324, 1988.

[24] B. Ismail, D. Ewing, J. S. Cotton, and J. S. Chang, "Characterization of the Soot Deposition profiles in Diesel Engine Exhaust Gas Recirculation (EGR) Cooling Devices Using a Digital Neutron Radiography Imaging Technique," *Trans. SAE Fuel and Lubrication*, vol. SAE 2004-01-1433, pp. 719-729, 2005.

[25] B. Ismail, D. Ewing, J. S. Chang, J. S. Cotton, "Development of a Non-destructive Neutron Radiography Technique to Measure the Three Dimensional Soot Deposition Profiles in a Diesel Exhaust System," *J. Aerosol. Sci.*, vol. 35, pp. 1275-1288, 2004.

[26] J. S. Chang and A. Watson, "Electromagnetic Hydrodynamics," *IEEE Trans. Electrical Insulation*, vol. 1, pp. 871-895, 1995.

[27] K. Jogan, A. Mizuno, T. Yamamoto, J. S. Chang, "The effect of residence time on the CO_2 reduction from combustion flue gases by an AC ferroelectric packed bed reactor," *IEEE Trans. IAS*, vol. 29, pp. 876-881, 1993.

[28] I. Maezono, J. S. Chang "Reduction of CO2 from combustion gases by dc corona torches," *IEEE Trans. IAS*, Vol. 26 (1990), 651-655.

[29] M. Higashi, M. Sugaya, K. Ueki, and K. Fujii, "Plasma Processing of Exhaust Gas from a Diesel Engine Vehicle", in *Proc. Int. Conf. on Plasma Chem.*, vol. 2, pp. 366-371, 1985.

[30] N. Boukhalfa, A. Goldman, M. Goldman, R. S. Sigmond, "CO_2 to CO Conversion in Corona Discharge," in *Proc. Int. Symp. on Plasma Chem.*, vol. 2, pp. 787-792, 1987.

[31] J. S. Chang, C. Luthereau, E. dela Cruz, P. I. Khalaf, D. Brocilo, G. D. Harvel, D. Ewing, N. A. Debacher, F. McCluskey, J. S. Cotton, and M. Bardeleben, "Plasma Diesel Soot Oxidation/Removal Characteristics by a Flow Stabilized Pulsed Corona Discharge Radical Injection System," *6th Conference of the French Electrostatics Society SFE 2008*, pp. 330-334, 2008.

[32] H. Matzig, "Chemical kinetics of flue gas cleaning by irradiation with electrons," *Adv. Chem. Phys.*, vol. 80, pp. 315-402, 1991.

[33] J. S. Chang, "The role of H_2O on the formation of NH_4NO_3 aerosol particles and De-KO, under the corona discharge treatment of combustion flue gases," *J. Aerosol Sci.*, vol. 20, pp. 1087-1090, 1989.

[34] J. S. Chang and J. S. Kwan, 1998 ESA-IEJ Joint Symp. On Electrostatics, J M Crowley and K Asano, Ed. Morgan Hill: Laplacian Press, 1998, pp. 390–408.